

ECONOMIC PROFITABILITY AND ENVIRONMENTAL IMPACT FOR THE INSTALLATION OF A COGENERATION SYSTEM IN AN AFRAMAX OIL TANKER

Marcelo Mora Moreira (I)* & Germán de Melo Rodríguez (II).

(I) Barcelona School of Nautical Studies of Barcelona (FNB), Doctoral student. Pla de Palau, 18, 08003 Barcelona, Spain

(II) Barcelona School of Nautical Studies of Barcelona (FNB), Director of Shipping business. Pla de Palau, 18, 08003 Barcelona, Spain

*Correspondence author: maalmorac@hotmail.com.

Abstract:

Nowadays, maritime transport has many challenges. Fuel consumption is necessary to make work the main and auxiliary systems, electrical and electronic equipment. However, during the process of consumption part of the thermal energy is not used, contributing to environmental impacts. In this context, ships share the concern, and to illustrate this, it is performed an “Economic Profitability and Environmental Impact for the Installation of a Cogeneration System in an Aframax Oil Tanker”. From the exhaust gases and implementing thermodynamic techniques it is possible to know the amount of recoverable energy using a gas turbine, steam or combined cycles. The feasibility of its application is based on the fuel saved by not using the auxiliary engines totally or partially, and evaluating in a period of 15 years through financial indexes. Finally, knowing the fuel savings, it is demonstrated how many of air pollutants (CO₂, NO_x, SO_x and PM) would be avoided for installing the cogeneration system.

Keywords:

Cogeneration, WHRS, PTG, STG, economic profitability, air pollutants.

NOMENCLATURE

Letter symbols

T	Temperature, K or °C
η_t	Isentropic efficiency
η_b	Boiler efficiency

\dot{m}_{bypass}	Mass flow of gas through bypass, kg/s
T_{bypass}	Gas temperature after combustion, K
$\dot{m}_{\text{g,turbo}}$	Mass flow of gas after turbo, kg/s
T_{turbo}	Gas temperature after turbo, K
$\dot{m}_{\text{g,total}}$	Total mass flow of gas after combustion, kg/s
P	Pressure (bar)
V	Volume (m ³)
P_{gt}	Gas turbine output, kW
c_p	Heat capacity at constant pressure, kJ/kg.K
h	Specific enthalpy, kJ/kg
P_{st}	Steam turbine (HP and LP) output, kW
\dot{m}_{v_H}	HP steam mass flow, kg/s
\dot{m}_{v_L}	LP steam mass flow, kg/s
$\dot{m}_{\text{g,bal.}}$	Total mass flow before HRB, k/s
$T_{\text{bal.}}$	Gas temperature before HRB, K
$T_{\text{g}_o,H}$	Gas temperature after HP economizer, K
\dot{m}_{v_H}	Mass flow of HP steam, kg/s
$h_{\text{v}_s,H}$	HP steam enthalpy in superheater, kg/s
$h_{\text{w}_p,H}$	HP water enthalpy in preheater, kg/s
$T_{\text{g}_i,L}$	Gas temperature after LP superheater, K
$T_{\text{g}_o,L}$	Gas temperature after LP economizer, K
$h_{\text{v}_s,L}$	LP steam enthalpy in superheater, kg/s
$h_{\text{w}_p,L}$	LP water enthalpy in preheater, kg/s
N_i	Indicated power output, kW
D	Displacement, ton
V	Speed, knots
C_a	Admiralty coefficient
I_i	Cash inflow, \$
O_i	Cash outflow, \$
I_o	Initial investment, \$

Acronyms:

NPV	Net present value
DR	Discount rate
IRR	Internal rate of return
CO ₂	Carbon dioxide
NO _x	Nitrogen oxides
SO _x	Sulphur oxides
PM	Particulate matter
WHB	Waste heat boiler
WHRS	Waste heat recovery system
SMCR	Specified maximum continuous rating

PTG	Power turbine generator
STG	Steam turbine generator
ICE	Internal compression engine
GHG	Greenhouse gases
SED	Specified emission data

Greek letters:

σ	Pressure ratio
γ	Heat capacity ratio

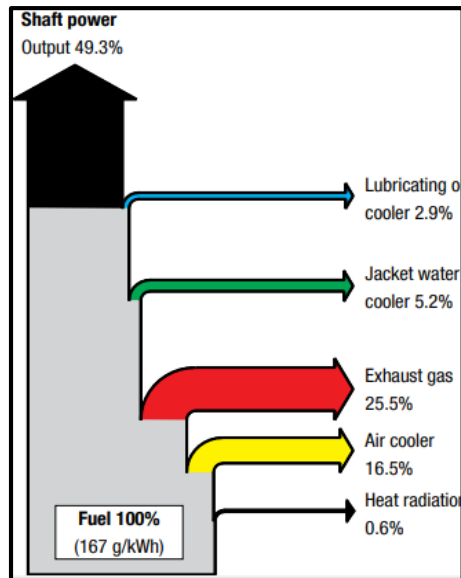
1. INTRODUCTION

1.1 BACKGROUND

The potential use of waste heat or energy contained in exhaust gases produced by the combustion in an ICE has been investigated for decades through cogeneration systems. Low fuel prices and high production costs have caused that WHRS are economically unattractive, despite the fact of contributing to the reduction of environmental impact. In addition, the lack of confidence of shipowners and the volatility of the maritime transport market have influenced in the development of this technology. On the other hand, the environmental standards by the use of cleaner fuels may cause the surge of WHRS.

Two-stroke low-speed marine engines are the most used propulsion machines in maritime transport. Most of waste energy of fuel used is contained in exhaust gases; its temperature is relatively low and with considerable mass flow, but, powerful enough to produce additional work through a cogeneration cycle.

Figure 1. Heat balance for a MAN 12S90ME-C9 engine.



Source: (MAN, 2014).

Energy optimization seeks all possible alternatives to improve efficiency, reduce costs and environmental impact. Nowadays, to recover the unused energy from the fuel, three aspects can be attacked:

- Cooling jackets and lube oil cooling
- Air cooling
- Exhaust gases

In a study undertaken by (MAN, 2014), the available energy in the fuel after combustion is disaggregated using a Sankey diagram, *figure 1*. It was shown that 25.5 % of the total energy is wasted through the exhaust gases, 16.5 % by air cooling, 5.2 % for cooling jacket and 2.9 % for the oil cooling. Citing the MAN 12K98MEC / MC 69,640 kW engine as an example, when it operates at 85 % SMCR, supplies about 58,344 kW. Over a period of 280 days a year and 24 hours a day, there are losses of 31,726 tons of fuel through exhaust gases, jacket waters, air intake and lube oil.

Energy optimization seeks all possible alternatives to improve efficiency, reduce costs and environmental impact. Nowadays, in order to recover the unused energy from the fuel, three aspects can be attacked:

1.2 PREVIOUS WORKS

Related to ship efficiency in ships in applying new technologies such as WHRS, there are a moderate amount of researches develop. (Baldi and Gabriellii, 2015) propose a method to calculate the amount of useful power that can be recovered. The results give a reduction of fuel consumption from 4% to 16% for a Panamax chemical/product tanker with two four-stroke Diesel engines rated 3840 kW each; (Liu *et al.*, 2020) propose a new type of WHRS based on the single steam Rankine cycle (SRC) and organic Rankine cycle (ORC) to utilize the heat of the exhaust gases and jacket cooling of a two-stroke marine engine. the results show that the ORC recovers more waste heat of the exhaust gases than the SRC; These results are consistent with a similar research for a container vessel which have a continuous rating (MCR) of 10,126 kW done by (Nielsen, Haglind and Larsen, 2014). Utilizing a ORC after the conventional waste heat recovery system is able to increase the combined cycle thermal efficiency by 2.6%; (Senary *et al.*, 2016) choose to study the application of WHRS in a Liquefied Nature Gas Carrier with 3 dual fuel engines. In addition to demonstrate that thermal efficiency increases, they concluded that Nitrogen Oxide and Carbon dioxide emissions reduce in 36.28% and 16.88% respectively; (Lampe *et al.*, 2018) proposes a novel method that can be used to predict the operational savings and costs of a WHRS; (Kyriakidis *et al.*, 2017) presents a model of a waste heat recovery system for a two-stroke marine diesel engine, but they include in the research, an integrated exhaust gas recirculation system in order to reduce NO_x emissions; (Shu *et al.*, 2017) present a thermal-economic analysis based on the ship's operational profile of a passenger cruise ship. They concluded that not all organics fluid can satisfy the payback limit; (Baldasso *et al.*, 2020) presents a novel and energy-efficient way to supply zero-emission power during harbor stays of marine vessels through the use of a thermal energy storage (TES) and a waste heat recovery system based on the organic Rankine cycle technology. The results prove that TES gives a lower cost of electricity than the battery systems; (Mohammed *et al.*, 2020) study a bulk carrier with an engine power (MCR) of 10,100 kW. The results showed that using ORC would decrease fuel consumption by 2.1 ton/day; (Mondejar *et al.*, 2017) present the quasi-steady state simulation of a regenerative organic Rankine cycle (ORC) integrated in a passenger vessel. They proved that approximately 22% of the total power demand on board is supplied by the WHRS; (Ma, Yang and Guo, 2012) perform a Thermodynamic and economic analyses of a WHRS Combined Turbine. Thermodynamic results indicate that it is possible to recover 5066 kW. On the other hands (Lümmen *et al.*, 2018) use the ORC in a 900 kW fast passenger ferry Diesel. They concluded that the transit is too short for recovering enough waste energy from the exhaust gases and its limitations in the use of WHRS.

2. COGENERATION IN SHIPS

According to (Fukugaki, 1994), new technologies were developed with the purpose of recovering the highest possible energy from the exhaust gases, using the recovered heat efficiently and reducing the consumption of electricity and steam. In chronological order, the cogeneration systems developed through the years are described as follows:

- 1978: Dual pressure system

- 1982: Dual pressure system with mixed pressure turbine
- 1984: Steam and hot water system with flash steam turbine
- 1986: Combined steam and gas turbine generator

2.1. NEED FOR COGENERATION IN SHIPS

The maritime transport is the foundation of the world economy; it is well known that cargo carried on sea is made by 70,000 merchant ships that cover the carriage of around 90 % of world trade. In addition, maritime transport is the most environmentally-friendly, from the perspective of GHG, something similar to the concept of economy of scale, merchant ships have the lowest emissions ratio of CO₂ per ton of cargo transported.

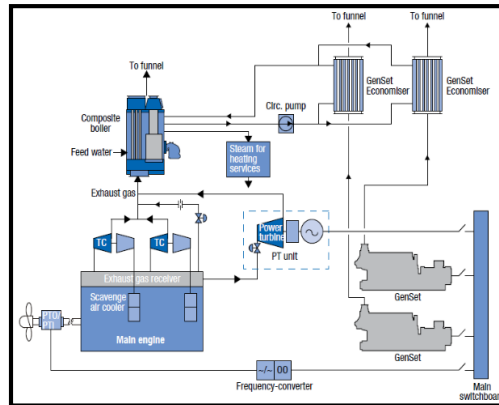
Furthermore to CO₂, air pollution generated in maritime transport comes primarily from SO_x, NO_x, and PM. According to (Neef and Box, 2009), shipping accounts for 15 % of global NO_x emissions (more than all cars, buses and trucks combined), between 2 and 3 % of CO₂ and between 3 and 7 % of SO_x of Global production. According to (Cormack, 2018), Global shipping emissions are predicted to increase by between 50 and 250 % by 2050, depending on future economic and energy developments.

These results prove the alarming of situation and the need for crucial measures to be adopted on the way of new technologies. For that reason, studies have been carried out for the fuels used and continuous improvement in the energy efficiency, with mandatory standards, based on national and international legislation. Technical solutions can be applied, such as scrubbers to reduce environmental impact, or reduce fuel consumption through the Ship Energy Efficiency Managements Plan (SEEMP) and besides the application of new technologies such as the use of WHRS.

2.2. TYPES OF WASTE HEAT RECOVERY SYSTEMS

PTG is gas drive turbine, installed in the exhaust gas bypass. The construction of the power turbine is based on turbocharger design, with some modifications in the support bearings and axis.

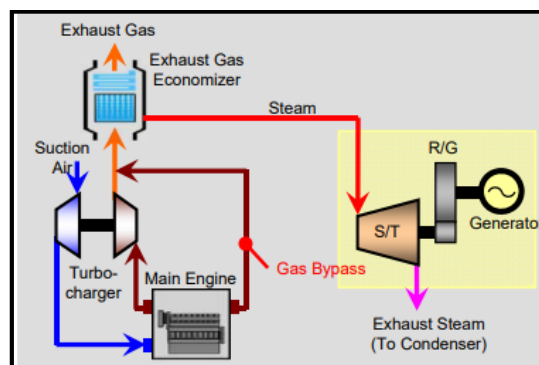
Figure 2. Schematic diagram of PTG-WHRS.



Source: (MAN, 2014).

In most cases the exhaust gas pipe system of the main engine is equipped with a boiler system. With this boiler, some of the energy in the exhaust gas is utilized to produce steam for use on board. Thus, with *STG (figure 3)* is possible to produce more steam and recover 5 to 8 % of waste energy. The steam turbine can either be a single or dual pressure, depending on the size of the system.

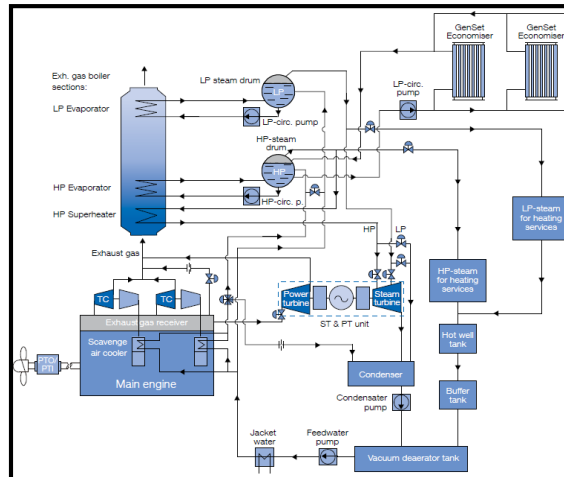
Figure 3. Schematic diagram of STG-WHRS.



Source: (MHI-MME, 2016).

In the case that the demand for electricity on board a ship is high, such as a container ship, the power turbine and steam turbine can be built together. The power turbine and the steam turbine is built onto a common bedplate and, via reduction gearboxes, connected to a common generator. A combined cycle, gas and steam scheme is shown in *Figure 4*, in which 8 to 11% SMCR power is recovered.

Figure 4. Schematic diagram of PT/ST-WHRS.



Source: (MAN, 2014).

2.3. MARITIME LAW

The IMO, a specialized agency of the United Nations, is the global authority for the regularization of pollutant emissions from maritime transport. The agreement that regulates the prevention of pollution from ships is MARPOL 73/78, and related to this research is involved the Annex VI about to the prevention of air pollution.

As a result of three years examination, MEPC 58 (October 2008) adopted the revised MARPOL Annex VI, which entered into force on 1 July 2010, limits the main air pollutants contained exhaust gases, including CO₂, SO_x and NO_x. Then, in short, the most relevant aspects of the regulatory control of emissions are:

CO₂. - Due to uncontrolled increase in CO₂ emissions caused by world's fleet of ships, the IMO decided to adopt two energy efficiency measures: the Energy Efficiency Design Index (EEDI) and the Ship Energy Efficiency Managements Plan (SEEMP).

NO_x. - Marine engines are required for testing, recognition and certification, in order to comply with NO_x emission limits. Under MARPOL Annex VI, this applies to marine diesel engine of over 130 kW, ships constructed after 1 January 2000 and like those that have undergone a major conversion.

SO_x. - MARPOL convention, as described its articles, there are Sulfur Emission Control Areas (SECAs). However, as regards the maximum SO_x allowed, this has been progressively reduced. The IMO has decided to regulate sulphur limit fuels at 0.50 % mass by mass from 2020, as against the current 3.5%.

3. CASE STUDY

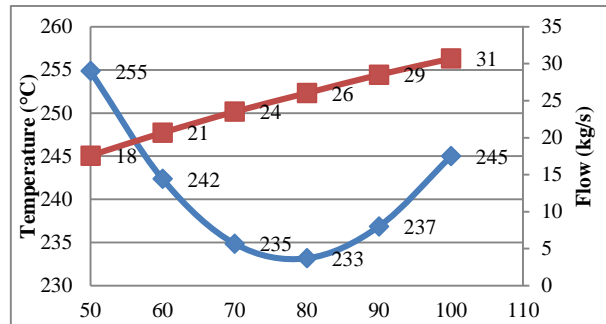
An Aframax oil tanker with keel laying 2010 is selected for this study. *Figure 5* specifies the dimensions and specifications. The aim of the research is to know the economic feasibility and pollutant emission reduction by the implementation of the cogeneration system. This is divided into three parts. First, using thermodynamic techniques for gas turbine, steam or combined cycle with different load operation, from 50 to 100 % SMCR, it is possible to know the usable energy contains in the exhaust gases. Second, based on the operational profile and marine navigation at different speeds, it is possible to know the actual remaining capacity. Finally, translated into economic terms the recovered kWe, an economic analysis is carried out in the remaining 15 years of operation.

Figure 5. Technical specifications of the Aframax oil tanker.

Specifications	Data
Length (m)	244
Beam(m)	42
Draft (m)	15
Dead weight (t)	105,310
Gross tonnage (GT)	62,400
Net tonnage (NT)	32,926
Speed (knots)	15
Output (HP)	16,360

The main engine has an output of 11,900 kW and uses fuel with a heating value of 42,700 kJ/kg. In addition, the exhaust gas production reaches a flow of 31 kg/s and temperature of 518 K. However, as shown in the *figure 6*, the study is carried out in 6 different power states: 50, 60, 70, 80, 90 and 100% SMCR.

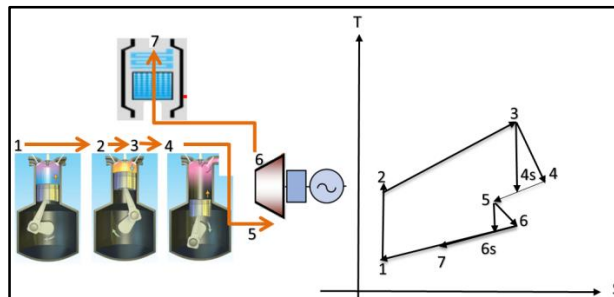
Figure 6. Variation of the exhaust gas flow (blue line) and temperature (red line) of a MAN B&W S60MC-C8 engine



3.1. THERMODYNAMIC MODEL OF THE GAS CYCLE

The main engine produces exhaust gases with a certain mass flow and temperature, however, not all gas goes directly to the power turbine, the most is necessary to drive the turbochargers. Then, from a starting point of a diesel and gas turbine cycle, the fluid behaves as it is shown in *Figure 7*.

Figure 7. Thermodynamic configuration of a diesel and Turbine expansion.



The thermodynamic transformations of diesel cycle and turbine expansion are specified as follows:

- 1-2: Isentropic compression of air (ICE);
- 2-3: Constant pressure heat transfer to air (ICE);
- 3-4: Isentropic expansion (ICE);
- 4-5: Expansion of gas before reaching the turbine;
- 5-6: Isentropic expansion in the gas turbine,
- 6-7: Heat transfer to a WHB;

7-1: Heat rejection to atmosphere.

As shown in **Figure 7**, from point 5 to 6 there is irreversibility. Then, **equation 1** defines the real enthalpy T_6 in relation to the gas efficiency turbine.

$$T_6 = T_5 - \eta_t \times (T_5 - T_{6s}); K \quad (1)$$

Equation 2 is applied to calculate the mass flow that drives the power turbine:

$$\dot{m}_{bypass} = \dot{m}_{gastotal} \times \%bypass; \frac{kg}{s} \quad (2)$$

The power supplied by the turbine is calculated using **equation 3**, product of the net work produced and the mass flow:

$$P_{gt} = \dot{m}_{bypass} \times cp \times (T_5 - T_6); kW \quad (3)$$

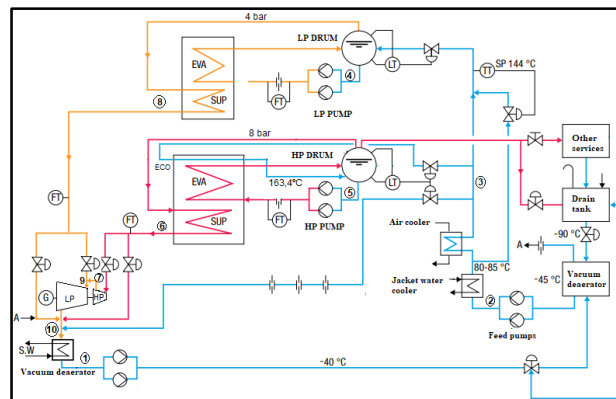
The temperature of the exhaust gas shown in the engine specifications is after the turbochargers. Then, the temperature of the exhaust gas before reaching the power turbine is calculated using **equation 4**,

$$T_5 = T_{6s} \times (\sigma)^{\frac{\gamma-1}{\gamma}} \quad (4)$$

3.2. THERMODYNAMIC MODEL OF THE STEAM CYCLE

The equations are obtained from a Rankine cycle with dual pressure. To understand the STG system shown in **figure 8** and for a better comprehension, the cycle is broken down into two bodies and each one with different stages as are shown in **figure 8**.

Figure 8. Schematic diagram of combined system with dual pressure.



Source: (MAN, 2014)

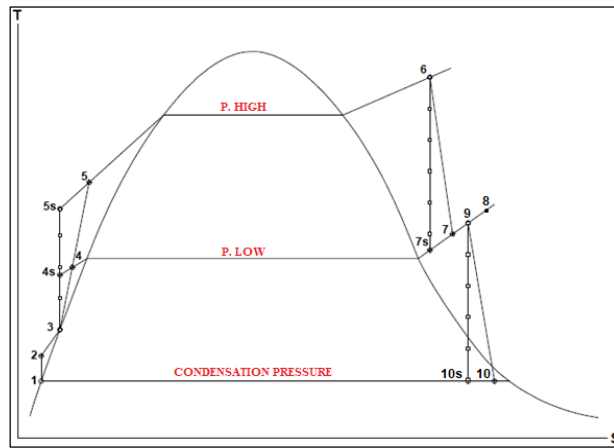
Then, starting from 1 to 2, water is pressurized, *equation 5* describes this part.

$$h_2 = h_1 + pv; \frac{kJ}{kg} \quad (5)$$

A steam cycle with this configuration, high and low pressure turbine, the power based on the net work done is calculated by *equation 6*.

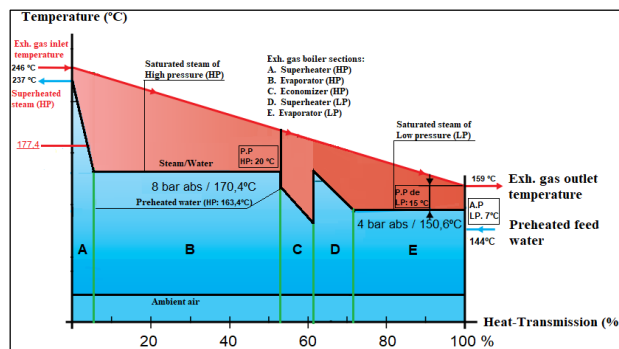
$$P_{st} = \dot{m}v_H \times (h_6 - h_7) + (\dot{m}v_H + \dot{m}v_L)(h_9 - h_{10}); kW \quad (6)$$

Figure 9. TS diagram of the STG system with dual pressure.



Using *figures 8 and 9*, it is possible to discern an energy-heat transmission diagram with dual pressure, *figure 10*.

Figure 10. Temperature-heat transmission diagram with dual pressure for a MAN B&W S60MC-C8 engine.



88 % of the total exhaust gases go to the turbochargers and the rest 12%, to steam generator. The gases coming from the turbochargers and the gases coming from the bypass are mixed, in order to obtain the thermal balance. *Equation 7* describes this phenomenon.

$$\begin{aligned} & \dot{m}g_{bypass} \times T_{bypass} + \dot{m}g_{turbo} \times T_{turbo} \\ & = \\ & \dot{m}g_{bal.} \times T_{bal.}; \frac{kg}{s} \end{aligned} \quad (7)$$

The power produced depends on the generation of steam in the high and low pressure sections. According to **Figure 9**, the exhaust gases release thermal energy to WHB, starting with the high pressure superheater (A) to the low pressure evaporator (E). Considering the divisions, a thermal balance can be done to calculate the mass flows of water and steam for the low and high pressure levels. First, from inlet gases to the exit of the high pressure economizer, heat is exchanged with the water or steam. **Equation 8** describes this segment.

$$\begin{aligned} & \eta_b \times \dot{m}g_{bal.} \times [cp \times (T_{bal.} - T_{g_{o.H}})] = \\ & \dot{m}v_H \times (hv_{s.H} - hw_{p.H.}); \frac{kg}{s} \end{aligned} \quad (8)$$

The energy balance equation for the LP section is:

$$\begin{aligned} & \eta_b \times \dot{m}g_{bal.} \times [(cp \times (T_{g_{i.L}} - T_{g_{o.L}}))] = \\ & \dot{m}v_L \times (hv_{s.L} - hw_{p.L.}); \frac{kg}{s} \end{aligned} \quad (9)$$

Finally, an energy balance is considered in the high turbine stage and in the mixing process that occurs with the LP steam, one coming from the low pressure (8) of the boiler and another coming from the HP turbine (7), until to get the balance (9) (see **equation 10**).

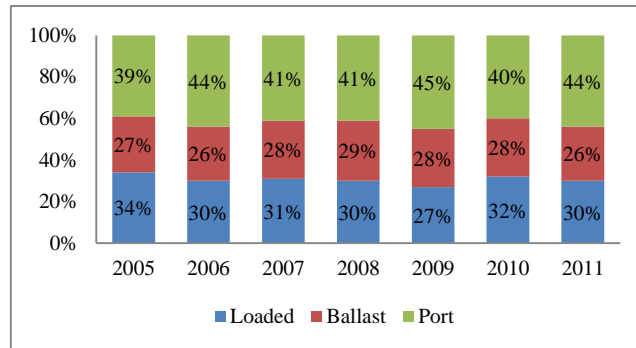
$$\dot{m}_8 h_8 + \dot{m}_7 h_7 = \dot{m}_9 h_9; \frac{kJ}{s} \quad (10)$$

3.3. OPERATIONAL PROFILE

WHRS operate as long as the ship is sailing, so there are three references when the ship is at sea: ship in port, ship in ballast and ship with cargo.

According to (6) the operation of an Aframax oil tanker varies among the references shown above. In addition, just as **figure 10** a ship of these characteristics spends the most time sailing, either in ballast or with cargo. The proportion between 2005 and 2011, delivers an average in load, ballast and port of 31, 27 and 42 % respectively, this means that within 365 days of the year an Aframax oil tanker sales 209 days, equivalent to 4,906 hours.

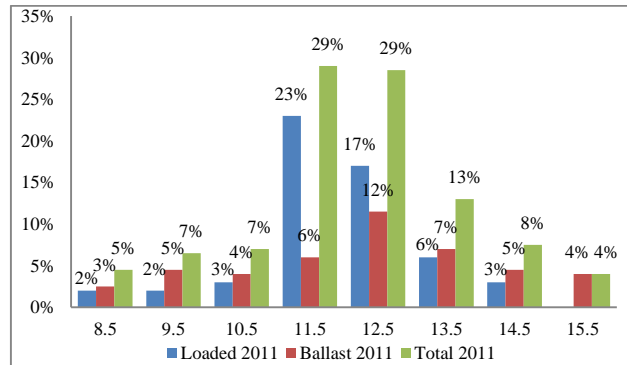
Figure 5. Operation profile of Aframax tankers in navigation and port during the period 2005 and 2011.



Source: (Banks *et al.*, 2013).

Additional information is taken from (6) to have a more precise relationship, **figure 12** shows speed as percentage during sailing.

Figure 12. Sailing in ballast and cargo condition of Aframax oil tankers in relation to speed during 2011.



Source: (Banks *et al.*, 2013)

To obtain the output in relation to speed, the admiralty formula is used.

$$N_i = \frac{D^{2/3} \times V^3}{C_a} \times 0.7457; kW \quad (11)$$

3.4. FINANCIAL INDEXES

Economists evaluate the profitability of investment projects using the Net Present Value (NPV). This is a method applied to determine the current value of all future cash flows through a Discount Rate (DR), as it is understood in the *equation 12*.

$$NPV = \sum_{i=1}^n \frac{I_i - O_i}{(1 + DR)^i} - I_0; \$ \quad (12)$$

Another method of profitability is to use the Internal Rate of Return (IRR). It is an interest rate that sets the NPV equal to zero. If the IRR is higher than the DR, it follows that the project is profitable.

3.5. POLLUTION REDUCTION

The emissions are the product of fuel consumption and the energy efficiency. To know the reduction of CO₂, SO_x, NO_x y PM the *equation 13* have to be applied.

$$ER = SED \times WHRS_{output} \times N_{time}; tons \quad (13)$$

4. RESULTS AND DISCUSSIONS

The results will mainly depend on which WHRS is used, either through a gas, steam or combined system. The analysis is based on a separate study of its two main components: steam and gas turbine.

4.1.COMPARISON OF SYSTEMS

The PTG, STG and combined systems, with an operational profile of 80 % SMCR, provide energy in 2.24, 5.39 and 7.54 % respectively.

Figure 6. WHRS recovery output data for an Aframax oil tanker with a MAN B&W S60MC-C8 engine.

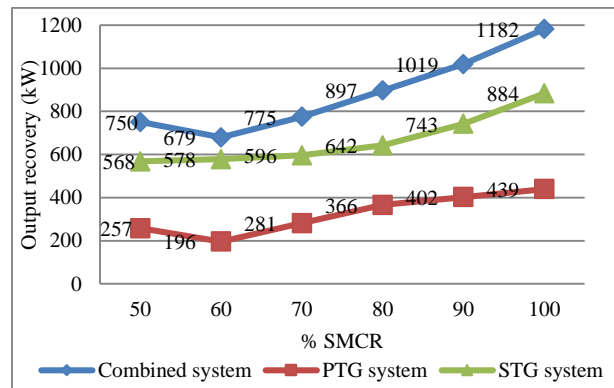


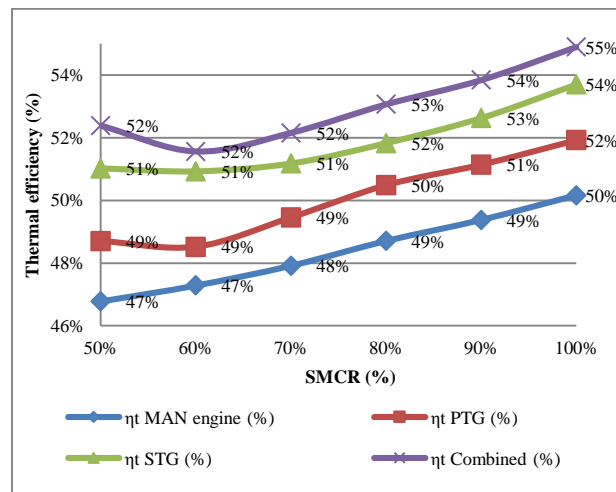
Figure 13 shows the heat recovery capacity of the three systems studied between the ranges of 50 to 100 % SMCR. In the case of 100 % SMCR, the difference from one system and the other

is around 400 kW. To get a clearer idea, this represents the power that 40 high-consumption homes need.

4.2. HEAT EFFICIENCY

The efficiency of two-stroke diesel engines has increased considerably in recent years, up to 50%. For the MAN B&W S60MC-C8 engine, the efficiency at different operational loads with and without WHRS is shown in *Figure 14*.

Figure 7. MAN B&W S60MC-C8 engine efficiency with and without WHRS.



4.3. CONSTRUCTION COSTS

The components needed for the WHRS system take up some space in the engine room, which have to be considered in the overall machinery arrangement. The rearrangement increases space requirements in engine room and optimization of the existing rooms (Nielsen, Mech and Sc, 2009)

In addition to above, there is a penalty of weight, including rebuilding of casing, decks in engine rooms, cables, pipes and structural elements. Even a combined cycle system has a length, width and height of 11, 4, and 5 meters respectively, with a weigh of 115 tons. This unit has to be installed within 50 meters in length that has an engine room of an Aframax oil tanker. The WHRS unit for the Aframax oil tanker is composed of the components shown in *figure 15*.

Figure 15. Construction, operation and maintenance costs of WHRS for an Aframax Oil tanker.

STRUCTURAL REARRANGEMENT		
General Description		Cost
-Ship repair works (plating, structural elements, pipes, cables, paint, and others) -Drawing plans and approval -Supervision: owner, SSCC, FLAG state	PTG System	\$150,000
	STG System	\$200,000
	Combined System	\$300,000
COGENERATION SYSTEM - WHRS		
General Description		Cost
STEAM TURBINE -Multiple stage reaction design, -Turbine casing of cast design, -Guide blade carriers of cast or forged design, -Emergency stop armature and control armature -Steam strainer -Gland steam system and turbine drainage system, -Rotor turning device, -Thermal insulation consisting	Combined System	\$499,396
EXHAUST GAS TURBINE (POWER TURBINE) -Variable inlet area geometry (VTA), -Thermal insulation		
PARALLEL SHAFT GEARBOX 3-PHASE 4-POLE SYNCHRONOUS GENERATOR -Out feed and star point box, -Brush-less excitation system, -Automatic voltage regulator, -Single air/water cooler	STG System	\$1,004,373
COMBINED OIL SYSTEM -Oil tank integrated in package base frame, -Single water-cooled oil cooler, -LPS for lubrication with mechanical and electrical pump, -Lubrication oil filters, -HPS for control with electrical pump, -Control oil filters.		
COMMON BASE FRAME PACKAGE CONTROL CUBICLE -Package control system, -Package supervisory equipment, -Package protection equipment, -Automatic synchronizing equipment, -Power management system for package	Combined System	\$1,343,728
MEASURING AND CONTROL CABLE WATER COOLED CONDENSER		
Total cost PTG System		\$649,396
Total cost STG System		\$1,204,373
Total cost combined system		\$1,643,728

Source: (Nielsen, Mech and Sc, 2009; Polo, Carlier and Seco, 2016).

The shipyard together with the manufacturer would work to install the different components. **Figure 15** shows the work that the shipyard must attend, such as dismantling, welding, materials handling and services. On the other hand, the ship owner together with the surveyor must redesign the structural and distribution plans for their approval by the maritime authority, as well as supervise the work in the shipyard. The cost for the shipyard fees has been assumed is reference to the annual maintenance cost of an Aframax oil tanker. Then, the costs reach for the PTG, STG and combined systems are 0.15, 0.20 and 0.30 M\$ respectively.

According to (Nielsen, Mech and Sc, 2009), the installation of a combined WHRS costs 1,137 \$/kW. This information is approximated with the facilities of cogeneration plants on land. Then, for a PTG, STG and combined system the cost would reach 0.5, 1.00 and 1.34 M\$ respectively.

Finally, the initial investment to install the WHRS is shown in *table 2*. In an Aframax oil tanker would be invested for the PTG, STG and combined system 0.65, 1.20 and 1.64 M\$ respectively.

4.4. FINANCIAL STUDY

As a starting point, revenues depend exclusively on the amount of fuel that is not used due to implementing cogeneration.

Figure 16. Fuel saving for using cogeneration - WHRS in an Aframax Oil Tanker.

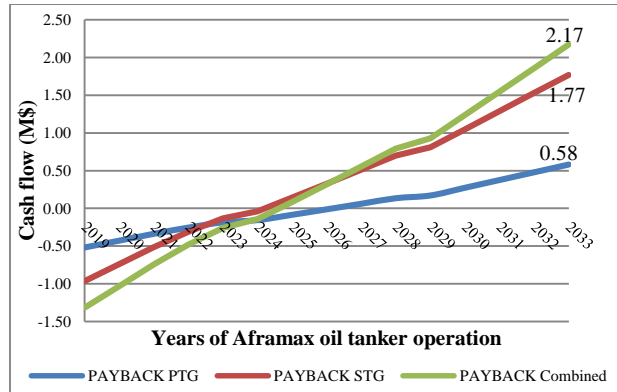
Speed (knots)	SMCR (%)	PTG (kW)	STG (kW)	Combined (kW)	SFOC (g/kW.h)	Sailing (hours)	Fuel saving PTG (\$)	Fuel saving STG (\$)	Fuel saving C (\$)
8.5	N/A	N/A	N/A	N/A	N/A	221	N/A	N/A	N/A
9.5	N/A	N/A	N/A	N/A	N/A	319	N/A	N/A	N/A
10.5	N/A	N/A	N/A	N/A	N/A	343	N/A	N/A	N/A
11.5	50	257	568	750	195	1423	35705	78775	104097
12.5	60	196	578	679	195	1398	26754	78830	92589
13.5	80	366	642	897	195	638	22757	39912	55750
14.5	100	439	884	1182	195	368	15761	31698	42408
15.5	100	439	884	1182	195	196	8406	16905	22617
							\$109,383	\$246,121	\$317,461

Assuming that the price of fuel oil is 500 \$/ton, the annual financial savings calculated for each system in the last three columns of *Figure 16* would be 0.11 M\$ (PTG), 0.25 M\$ (STG) and 0.32 M\$ (combined)

The cash flow shows the costs that correspond to the money needed for the operation and maintenance the WHRS. In general, these would be labor, spare parts, lubricants, training, and administrative costs.

Using the Payback, the recovery time of the investment is known through cash flow. Due to this, a graph (*figure 17*) in cash values over the operational years of the Aframax oil tanker is obtained. Then, the recovery time of the investment for the PTG, STG and combined system is 8, 6 and 5 years respectively.

Figure 8. Aframax oil tanker payback calculation for WHRS.



With cash flow for the 15 years of the Aframax oil tanker operation and a DR of 12 %, a positive NPV index is obtained for the three cogeneration systems. The second index, IRR, for the PTG, STG and combined system is 12.4, 18.6 and 17.0 % respectively. It means that both results are satisfactory.

4.5. ENVIRONMENTAL IMPACT

Using the SED, the output power of the WHRS and the navigation time, it is possible to know the reduction of polluting emissions (CO₂, SO_x, NO_x and PM). These results are shown in *figure 18*.

Figure 18. Emission reduction for using WHRS in an Aframax Oil Tanker.

SMCR (%)	PTG (t/year)				STG (t/year)				Combined (t/year)			
	CO ₂ (t)	NO _x (t)	SO _x (t)	PM (t)	CO ₂ (t)	NO _x (t)	SO _x (t)	PM (t)	CO ₂ (t)	NO _x (t)	SO _x (t)	PM (t)
50	201.4	6.2	3.8	0.7	444.3	13.7	2.1	1.6	587.2	18.2	11.0	2.1
60	149.1	4.7	2.8	0.5	439.3	13.7	9.8	1.6	516.0	16.1	9.8	1.9
80	126.7	4.0	2.4	0.5	222.1	7.0	5.9	0.8	310.3	9.7	5.9	1.1
100	89.9	2.7	1.7	0.3	180.8	5.5	4.5	0.7	241.9	7.4	4.5	0.9
100	48.0	1.5	0.9	0.2	96.4	2.9	2.4	0.3	129.0	3.9	2.4	0.5
	615	19	12	2	1383	43	25	5	1784	55	34	7

Currently, many industry projects lead to environmental impact, shipping industry is no exception. The Marine Environment Protection Committee (MEPC) under IMO's remit is constantly working to improve the energy efficiency of ships and one of its main aims is to reduce the environmental impact. Even, if the cogeneration project is not profitable enough for shipping companies, the environmental benefits are significant, as shown in *figure 18*. Only the implementation of the PTG system can reduce CO₂ emissions by 615 tons per year.

4.6. COMPARABILITY OF RESULTS

The researches on these systems have increased in the last 10 year. Many authors develop model based on standard conditions for a specific engine or ship. But, they don't consider a real operational profile. To obtain the thermodynamic and economics results for the WHRS, a voyage plan is necessary. So, from this argument, a similar research was done by (Suárez de la Fuente, Roberge and Greig, 2017). The preselected design parameters and results obtained are compared in *the figure 19*.

Figure 19. Comparability of data across two Aframax oil tanker.

-	Related research	Actual research
Exhaust gas temperature to ambient (°C)	165	159
Operational profile (h)	5,100	4,906
WHRs type	Simple	Dual
Refrigeration Cooling jackets, lube oil cooling and air cooling	No	Yes
Pinch point (°C)	30	15
Fuel cost (\$)	703	500
Electrical Power output (kWe)	290	642
Fuel saving (\$)	155,000	246,121
CO ₂ emission reduction (t/year)	705	1,383
Initial investment (\$)	97,700	1,204,000

It can be seen that the results are different. For example, the fuel saving per year is higher than the related research. This is because the initial data are different such as: the pinch point, WHRS type (they use a single pressure system), exhaust gas temperature outlet and the heat from jacket, lube oil and air is not use.

5. CONCLUSIONS

Three types of cogeneration systems were evaluated in the Aframax oil tanker, using thermodynamic equations, design parameters such as Pinch and Approach Point, flow and temperature of the exhaust gases and output of the main engine between the ranges of 50 and 100 % SMCR. For an average output of 80 % SMCR, it is possible to increase the efficiency in the STG, PTG and combined system for about 2, 5 and 8 % respectively.

The electrical balance and operational profile of the Aframax oil tanker was obtained. The service hours of the main engine influence in the amount of fuel that can be saved in a year of operation. During the 365 days of the year, the Aframax oil tanker navigates a period of 4,906 hours. Then, it is affirmed that if the ship did not navigate enough hours to produce economic benefits, its installation would be exclusively to improve the environmental impact

The economic balance was made for a period of 15 years, the data needed are: the initial investment that consist in the structural configuration and WHRS installation, which cost is

1,137 \$/kW; the revenue, considered as incomes that help save 219 (PTG), 492 (STG) and 635 (Combined) tons of bunker; the production costs to maintain the productively, such as spare parts. Then, Based on expected cash flows, the payback for installing the PTG, STG and combined system would be in 8, 6 and 5 years respectively. In addition, introducing the investment risk, the financial profitability indexes NPV and IRR are acceptable during the remaining 15 years of the Aframax oil tanker.

Finally, using the waste energy from the exhaust gases the reduction of bunker would improve the environmental impact. Therefore, following this line CO₂, NO_x, SO_x and PM: for the PTG system, 615, 19, 12 and 2 tons per year are reduced; for the STG system, 1383, 43, 25 and 5 tons per year are reduced; and for the combined system 1,784, 55, 34 and 7 tons per year are reduced

References:

Baldasso, E. and others. Organic Rankine cycle-based waste heat recovery system combined with thermal energy storage for emission-free power generation on ships during harbor stays. *Journal of Cleaner Production*. [online]. 2020, No. 271, p. 122394. Online ISSN: 1879-1786. [Date of access: 29 July 2020]. Available at: <https://doi.org/10.1016/j.jclepro.2020.122394>

Baldi, F.; Gabriellii, C. A feasibility analysis of waste heat recovery systems for marine applications. *Energy* [online]. Elsevier, 2015, Vol. 80, p. 654–665. Online ISSN: 0360-5442. [Date of access: 29 July 2020]. Available at: <https://doi.org/10.1016/j.energy.2014.12.020>

Banks, C. and others. Understanding ship operating profiles with an aim to improve energy efficient ship operations. In: *Proceedings of the Low Carbon Shipping Conference*. London, 9 Sep 2013, p. 1–11.

Cormack, C. Shipping emissions predicted to rise by up to 250% by 2050. In: *Agrilands* [online]. Agriland Media, 2018. [Date of access: 16 July 2020]. Available at: <https://www.agriland.ie/farming-news/shipping-emissions-predicted-to-rise-by-up-to-250-by-2050/>

Fukugaki, A. Review of shipboard energy technology : thoughts and facts behind the scene. *Transactions The Institute of Marine Engineers*. London : Institute of Marine Engineers, Marine Management, 1994, Vol. 106.

Kyriakidis, F. and others. Modeling and optimization of integrated exhaust gas recirculation and multi-stage waste heat recovery in marine engines. *Energy Conversion and Management* [online]. Elsevier, 2017, Vol. 151, p. 286–295. Online ISSN: 1879-2227 [Date of access: 16 July 2020]. Available at: <https://doi.org/10.1016/j.enconman.2017.09.004>

Lampe, J. and others. Model-based assessment of energy-efficiency, dependability, and cost-effectiveness of waste heat recovery systems onboard ship. *Ocean Engineering* [online]. 2018,

Vol. 157, p. 234–250. Online ISSN: 1873-5258. [Date of access: 29 July 2020]. Available at: <https://doi.org/10.1016/j.oceaneng.2018.03.062>

Liu, X. and others. A novel waste heat recovery system combining steam Rankine cycle and organic Rankine cycle for marine engine. *Journal of Cleaner Production* [online]. Elsevier, 2020, Vol. 265, p. 121502. Online ISSN: 1879-1786. [Date of access: 29 July 2020]. Available at: <https://doi.org/10.1016/j.jclepro.2020.121502>

Lümmen, N. and others. Comparison of organic Rankine cycle concepts for recovering waste heat in a hybrid powertrain on a fast passenger ferry. *Energy Conversion and Management* [online]. Elsevier, 2018, Vol. 163, p. 371–383. Online ISSN: 1879-2227. [Date of access: 29 July 2020]. Available at: <https://doi.org/10.1016/j.enconman.2018.02.063>

Ma, Z.; Yang, D.; Guo, Q. Conceptual design and performance analysis of an exhaust gas waste heat recovery system for a 10000TEU container ship. *Polish Maritime Research* [online]. 2012, Vol. 19, No. 2, p. 31–38. Online ISSN: 2083-7429. [Date of access: 29 July 2020]. Available at: <https://doi.org/10.2478/v10012-012-0012-8>

MAN. *Waste Heat Recovery System (WHRS), reduction*

of fuel consumption, emissions and EEDI [online]. Copenhagen : Man Diesel & Turbo, 2014, 29 p. [Date of access: 29 July 2020]. Available at: <https://mandieselturbo.com/docs/librariesprovider6/technical-papers/waste-heat-recovery-system.pdf>

Mitsubishi Heavy Industries Marine Machinery & Engine. WHRS-STG : environment friendly and economical solutions : [Waste Heat Recovery for Container Vessels]. [online]. MHI-MME, 2016, 23 p. [Date of access: 29 July 2020]. Available at: https://www.mhi-mme.com/products/boilerturbine/WHRS_Presentation.pdf

Mohammed, A. G. and others. Performance analysis of supercritical ORC utilizing marine diesel engine waste heat recovery. *Alexandria Engineering Journal* [online]. Faculty of Engineering, Alexandria University, 2020, Vol. 59, No. 2, p. 893–904. [Date of access: 29 July 2020]. Available at: <https://doi.org/10.1016/j.aej.2020.03.021>

Mondejar, M. E. and others. Quasi-steady state simulation of an organic Rankine cycle for waste heat recovery in a passenger vessel. *Applied Energy* [online]. Elsevier, 2017, Vol. 185, part 2, p. 1324–1335. Online ISSN: 1872-9118. [Date of access: 29 July 2020]. Available at: <https://doi.org/10.1016/j.apenergy.2016.03.024>

Neef, D.; Box, P. O. *The development of a global maritime emissions inventory using electronic monitoring and reporting techniques*. Maryland: DNA Maritime LLC, 2009, p. 1–12.

Nielsen, B. Ø. *8500 TEU Container Ship Green Ship of the Future Concept study* [online]. Denmark : Odense Steel Shipyard, 2009, 74 p. [Date of access: 29 July 2020]. Available at: <https://www.dendanskemaritimefond.dk/wp-content/uploads/2016/04/Green-Ship-Report-Containership-4Dec09.pdf>

Nielsen, R. F.; Haglind, F.; Larsen, U. Design and modeling of an advanced marine machinery system including waste heat recovery and removal of sulphur oxides. *Energy Conversion and Management* [online]. Elsevier, 2014, Vol. 85, p. 687–693. Online ISSN: 1879-2227. [Date of access: 29 July 2020]. Available at: <https://doi.org/10.1016/j.enconman.2014.03.038>

Polo, G.; Carlier, M.; Seco, E. *Temas de Tráfico Marítimo Transporte Marítimo y Legislación : curso 2016-2017*. Madrid: Universidad Politécnica de Madrid, ETSIN, 2016.

Senary, K. and others. Development of a waste heat recovery system onboard LNG carrier to meet IMO regulations. *Alexandria Engineering Journal* [online]. Faculty of Engineering, Alexandria University, 2016, Vol. 55, No. 3, p. 1951–1960. [Date of access: 29 July 2020]. Available at: <https://doi.org/10.1016/j.aej.2016.07.027>

Shu, G. and others. Operational profile based thermal-economic analysis on an Organic Rankine cycle using for harvesting marine engine's exhaust waste heat. *Energy Conversion and Management* [online]. Elsevier, 2017, Vol. 146, p. 107–123. Online ISSN: 1879-2227. [Date of access: 29 July 2020]. Available at: <https://doi.org/10.1016/j.enconman.2017.04.099>

Suárez de la Fuente, S.; Roberge, D.; Greig, A. R. Safety and CO2 emissions: implications of using organic fluids in a ship's waste heat recovery system. *Marine Policy*. Elsevier, 2017, Vol. 75, p. 191–203. Online ISSN: 1872-9460. [Date of access: 29 July 2020]. Available at: <https://doi.org/10.1016/j.marpol.2016.02.008>